phys. stat. sol. (a) 123, 461 (1991)

Subject classification: 68.55 and 73.60; 78.65; 85; S10.15

Siemens AG, Corporate Research and Development, München[1])

Microstructure and Etching Properties of Sputtered Indium-Tin Oxide (ITO)

By

M. HOHEISEL, A. MITWALSKY, and C. MROTZEK

Indium-tin oxide (ITO) applied to optoelectronic devices must meet several requirements simultaneously, i.e. electrical conductivity, optical transparency, and structurability by photolithography. As will be shown, these properties are mainly based on the microstructure of the ITO films. The microstructure changes from amorphous to polycrystalline depending on the oxygen partial pressure in the sputtering ambient and the deposition rate. We investigated the influence of an oxide layer on the target surface, its removal prior to film deposition, and its formation during the sputtering process. The reproducibility of the ITO microstructure and the etching properties are discussed in detail.

Indium-Zinn-Oxid (ITO) für die Anwendung in opto-elektronischen Bauelementen muß gleichzeitig verschiedene Anforderungen erfüllen: elektrische Leitfähigkeit, optische Transparenz und Strukturierbarkeit mit Hilfe der Photolithographie. Wie in dieser Arbeit gezeigt wird, hängen diese Eigenschaften hauptsächlich vom Gefüge der Schichten ab. Es ändert sich von amorph zu polykristallin in Abhängigkeit vom Sauerstoffpartialdruck im Sputterraum und der Abscheiderate. Wir haben den Einfluß einer Oxidschicht auf der Target-Oberfläche, ihre Entfernung vor dem Sputtern und ihre Bildung während des Sputterprozesses untersucht. Die Reproduzierbarkeit des ITO-Gefüges und die Ätz-Eigenschaften werden ausführlich diskutiert.

1. Introduction

Transparent conductive materials are widely used in optoelectronic applications. Besides tin oxide and zinc oxide, which are used for solar cells [1], indium-tin oxide (ITO) commonly forms the transparent electrode of electro-optical devices, i.e. image sensors based on amorphous silicon (a-Si:H) [2, 3], photodiodes, and liquid-crystal displays [4]. A review is given in [5].

In large-area microelectronics, Schottky diodes consist of a-Si:H as the semiconductor and ITO as an electrode which is optically transparent in the visible spectral region. An intermediate silicon oxide layer enhances chemical stability and Schottky barrier height [6 to 8].

In our case of image sensors for facsimile applications the requirements are as follows:

(i) electrical sheet resistance less than 1 kΩ,

(ii) transparency in the visible spectral region (i.e. 400 to 700 nm) more than 80%,

(iii) etchability to enable device patterning by photolithography, and

(iv) reproducibility of the film deposition to assure a reliable mass production process.

Two principal methods are available for preparing ITO films, i.e. evaporation of ITO [9] or reactive sputtering of an indium-tin alloy in an argon-oxygen mixture. In this paper, we focus on the latter case. Sputtered ITO films were investigated by cross-sectional

[1]) Otto-Hahn-Ring 6, W-8000 München 83, FRG.

transmission electron microscopy (TEM) and X-ray diffraction (XRD). Additionally, we measured conductivity, transparency, and etching behavior to clarify the correlations between microstructure and these macroscopic properties.

2. Experimental

ITO films were deposited on glass substrates (Corning 7059) by reactive dc magnetron sputtering of a metallic alloy target, composed of 90% indium and 10% tin, in a Balzers BAK600 sputtering machine. The target size was $12.7 \times 43.2\ cm^2$ ($5'' \times 17''$), the dc power 750 W.

A base vacuum of less than 10^{-5} Pa was assured by means of a cryo pump. The gas used for sputtering was a mixture of 3×10^{-1} Pa Ar with up to 5×10^{-1} Pa O_2 added. ITO films were deposited up to a film thickness of about 100 nm. The substrates rotated during deposition at $20\ min^{-1}$ to produce homogeneous films over a large area. Heating of the substrates was thus not possible. The deposition temperature was room temperature (below 50 °C). Deposition at elevated temperature (above 130 °C) generally leads to polycrystalline ITO films [10].

During the sputtering process the target surface becomes oxidized. This alters the deposition rate [11] and thus the microstructure of the growing film. The oxide was removed prior to each sputtering run by pre-sputtering the target in a pure Ar ambient. As the input power is held constant, the target voltage can be monitored to control the sputtering conditions. Pre-sputtering was continued until a constant target voltage had been established. This procedure always leads to identical sputtering conditions and assures reproducible film growth.

Specimens were prepared for cross-sectional transmission electron microscopy (TEM) using standard procedures, i.e. two pieces were glued together front to front and slices were cut from this structure with a dicing saw. Mechanical grinding and polishing of the slices down to a thickness of about 5 μm provided large transparent regions after ion-beam thinning with argon ions. The TEM investigations were performed in a JEOL 2000 FX microscope using a beam voltage of 200 kV.

Etching of the samples was carried out in sulfuric acid or hydrochloric acid. Other (stronger) agents of the kind investigated by others [12, 13] may not be used, as they would destroy underlying structures of the devices in which ITO is to be applied. After producing a resist mask and wet etching in 5% H_2SO_4 or 5% HCl in H_2O, the patterned films were examined in a scanning electron microscope (SEM) [14].

Finally, the ITO samples were annealed for 1 h at 200 °C in an oxygen ambient or in air. This decreases the sheet resistance and enhances the transparency considerably.

3. Results

In our measurements we investigated several properties of the ITO films. The most important macroscopic properties were electrical conductivity, optical transparency, and etching behavior. They were correlated to the microstructure, which is itself determined by the sputtering conditions, i.e. sputtering ambient, rate, and target state before starting a sputter run. Therefore, investigations of the target surface were carried out as well.

3.1 Transparency and conductivity

The dependence of the optical transmission and the sheet resistance R of a series of ITO samples on the oxygen partial pressure $p[O_2]$ in the sputtering ambient are displayed in Fig. 1. The values were measured after annealing the samples as described above. With a low oxygen partial pressure ($p[O_2] \leqq 10^{-1}$ Pa), ITO films with a sufficiently low sheet resistance ($R \leqq 1$ kΩ) are obtained. Their transparency is rather poor, ranging from 20 to 50%. ITO films prepared at $p[O_2] \geqq 2 \times 10^{-1}$ Pa are highly transparent, i.e. >85%, but the resistance rises above 20 kΩ and may even reach values of the order 10 MΩ. The features in the curve of resistivity versus oxygen partial pressure are similar to those presented in [15]. A detailed investigation of the conduction mechanism was carried out by Dietrich [16].

ITO films designed for use in large-area microelectronics applications must fulfil the requirements listed above simultaneously. This is only possible in a narrow partial pressure range of oxygen around $p[O_2] = 1.6 \times 10^{-1}$ Pa. This requires very careful control of each sputtering parameter, which must be kept within quite close limits during the sputtering process. Every unintended influence on the sputtering machine thus causes poor reproducibility in ITO production.

A crucial factor which determines $p[O_2]$ is the balance between incoming O_2 flow, pumping speed, and O_2 consumption by the oxidation reaction leading to ITO [11]. This is a well-known problem in every reactive sputtering process, for instance, when producing TiN_x from a Ti target in a nitrogen ambient [17]. An oxidized target surface reduces the sputtering rate considerably, thus causing an increase in $p[O_2]$. Since target oxidation takes place during every sputtering run, some instabilities in process control can hardly be avoided. A theoretical calculation on this problem has been carried out by Larsson et al. [18]. Details of the processes on the target surface will be discussed below.

3.2 Microstructure of the ITO layers

The vertical structure of the ITO films can be observed directly with high spatial resolution (≈0.5 nm) by TEM bright-field images of thin cross-sections. In contrast to plan-view TEM, amorphous and crystalline parts of ITO specimens lying on top of each other can be easily distinguished.

A standard ITO layer ($p[O_2] = 1.6 \times 10^{-1}$ Pa) is shown in Fig. 2 and turns out to be completely amorphous in the lower part of the film. Polycrystalline growth starts at about half of the film thickness. The grains are mostly conically shaped, resulting in a large lateral extension at the ITO surface. There, the grain size is up to 50 nm. Simultaneously with the beginning of crystalline growth, channels of low density material approximately 1 nm in width form. They are situated predominantly at grain boundaries and show a honeycomb-like structure in plan-view specimens. During annealing (200 °C, 1 h, in O_2) a transformation takes place to a completely polycrystalline microstructure (Fig. 3). The vertical channels are increased in size and density. Extensive electron and X-ray diffraction measurements on several annealed ITO films always show up the formation of indium sesquioxide (In_2O_3) with cubic bixbyite crystal structure [19]. The formerly amorphous part must therefore be close to the stoichiometric composition of In_2O_3. Of course, the Sn doping performed was analyzed by energy-dispersive X-ray spectroscopy (EDX) in a TEM to be about 5% mole fraction with respect to In_2O_3, resulting in the well-known degenerate semiconducting behavior of ITO [5, 20]. In addition, the density of oxygen vacancies also plays a fundamental role for the conduction mechanism in ITO but was not further considered here.

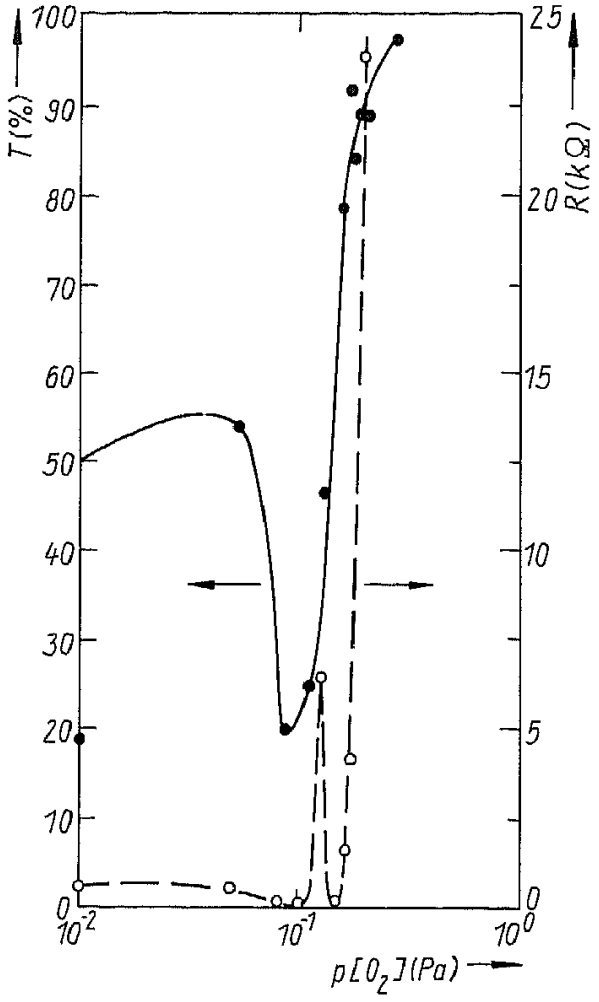

Fig. 1. Dependence of the optical transmission (———) and the sheet resistance R (— — —) of about 100 nm thick ITO films on the O_2 partial pressure during the sputtering process. ITO with good properties can only be produced in a narrow partial pressure range of O_2 around 1.6×10^{-1} Pa

The restricted reproducibility of ITO films at standard conditions ($p[O_2] = 1.6 \times 10^{-1}$ Pa) is demonstrated in Fig. 4 and is mainly due to the large gradients of the macroscopic data at this operating point (see Fig. 1). This ITO film is completely crystalline in contrast to the one of Fig. 2. Both samples have not been annealed. Corresponding macroscopic properties have changed, as will be summarized at the end of this chapter. For this sample, the pre-sputtering time had been reduced significantly compared to the film of Fig. 2. The target surface was consequently altered, resulting in a different sputter rate and slightly shifting the effective operating point. The influence of the sputter target on the deposition process will be discussed in detail in the next section. From this it can be concluded that the film preparation parameters have to be carefully checked to achieve high reproducibility in this narrow process window. One possible solution for stabilizing the deposition conditions is given in [21].

When leaving standard deposition conditions, an increase of oxygen partial pressure to $p[O_2] = 5 \times 10^{-1}$ Pa leads to a completely crystalline film with an approximately 20 nm thick compact bottom layer (Fig. 5a). The upper part of the ITO reveals pronounced columnar growth of ITO grains which are separated by the honeycomb-like channel system mentioned above. Some of these grains extend throughout the whole ITO film. Selected

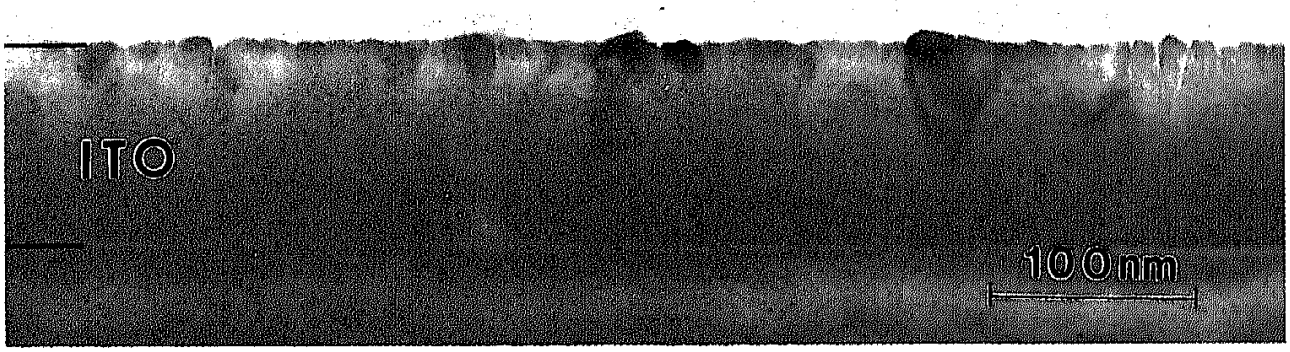

Fig. 2. TEM cross-section of an ITO film sputtered at $p[O_2] = 1.6 \times 10^{-1}$ Pa

Fig. 3. ITO film ($p[O_2] = 1.6 \times 10^{-1}$ Pa) after annealing for 1 h at 200 °C in O_2

area diffraction (SAD) of ITO on Si(100) substrate reveals a preferential ⟨222⟩ orientation of the film (Fig. 5b), i.e. the In_2O_3 crystal growth is determined by {222} lattice planes. A similar behavior was observed on many crystalline ITO films.

If we look at oxygen-poor sputter deposition ($p[O_2] = 0.1 \times 10^{-1}$ Pa), we note that the ITO film exhibits isolated grains about 30 nm in size (with In_2O_3 crystal structure) embedded in a porous amorphous phase (Fig. 6). The increase in deposition rate with decreasing oxygen partial pressure was not sufficiently compensated by reducing the sputter time and resulted in an abnormally thick ITO layer. The amorphous part of the film consists of oxygen-poor ITO, as was found by electron probe microanalysis.

The interaction of the etching agent used with ITO is shown in Fig. 7. Starting from a completely crystalline ITO film (as in Fig. 3, 4 or 5), after prolonged exposure to HCl a very resistant compact polycrystalline layer, nearly 20 nm in thickness, remains on the substrate. Most of the grains in the upper part of the ITO film were underetched and lifted off by the acid penetrating into the vertical pores and by lateral etching. Isolated larger grains extending throughout the whole ITO layer could not be removed and their remains are visible in Fig. 7. It was found for a series of ITO films that amorphous and porous polycrystalline materials reveal good or sufficient etchability, whereas compact polycrystalline ITO is very resistant to the etching agents used for this application.

The other macroscopic properties, namely optical transmission and sheet resistance, can also be correlated with the microstructure of ITO for the investigated process window. The oxygen-poor films with their mostly amorphous microstructure containing a small number of grains exhibit high electrical conductivity with very poor optical transmission. Intermetallic amorphous phases are probably responsible for these properties. With increasing oxygen

Fig. 4. The restricted reproducibility of ITO film fabrication ($p[O_2] = 1.6 \times 10^{-1}$ Pa) is demonstrated by the different microstructure compared to Fig. 2

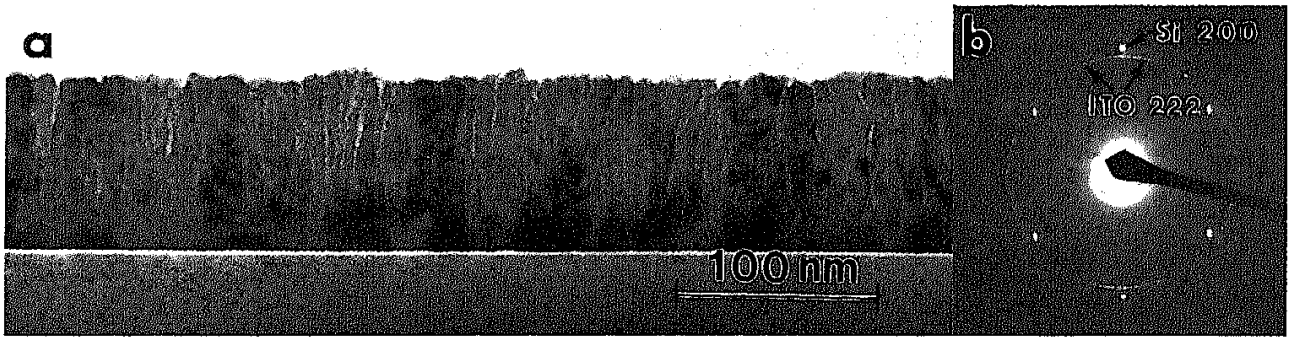

Fig. 5. a) TEM cross-section of an ITO film sputtered at $p[O_2] = 5 \times 10^{-1}$ Pa and b) SAD pattern of this ITO film on a Si(100) substrate

concentration, ITO becomes crystalline with intermediate conductivity and high optical transmission. Polycrystalline films with a lot of vertical pores in particular exhibit low conductivity combined with intermediate optical transmission.

3.3 Target oxidation

The state of the target surface turned out to be the crucial factor for the whole ITO fabrication process [10]. First of all, a surface oxide layer alters the sputtering rate. Since the oxide has a higher resistivity than the metal target, the target current drops with increasing surface oxide layer thickness. In parallel to this, the target voltage rises and the deposition rate will decrease accordingly.

Magnetron sputtering leads to non-uniform target erosion that causes an oval crater during the lifetime of the target. Analysis of a used-up target elucidates the process of target oxidation in detail. Inside the crater, the oxide can be removed by pre-sputtering in pure Ar, but bombardment by oxygen ions during the sputtering run causes fast oxidation. By repeated sequences of oxidation and oxid removal, a very rough target surface emerges on the bottom of the crater, as can be seen in the SEM image of Fig. 8a. The target surface outside the crater was oxidized completely during its lifetime (Fig. 8b). There, the oxide thickness amounts to about 600 nm, as was measured by Auger electron spectroscopy (AES) [22]. The roughness corresponds to the final mechanical treatment during target production.

Monitoring the target voltage has proved to be a simple method of maintaining a reproducible state of the target surface. During pre-sputtering, the target voltage drops

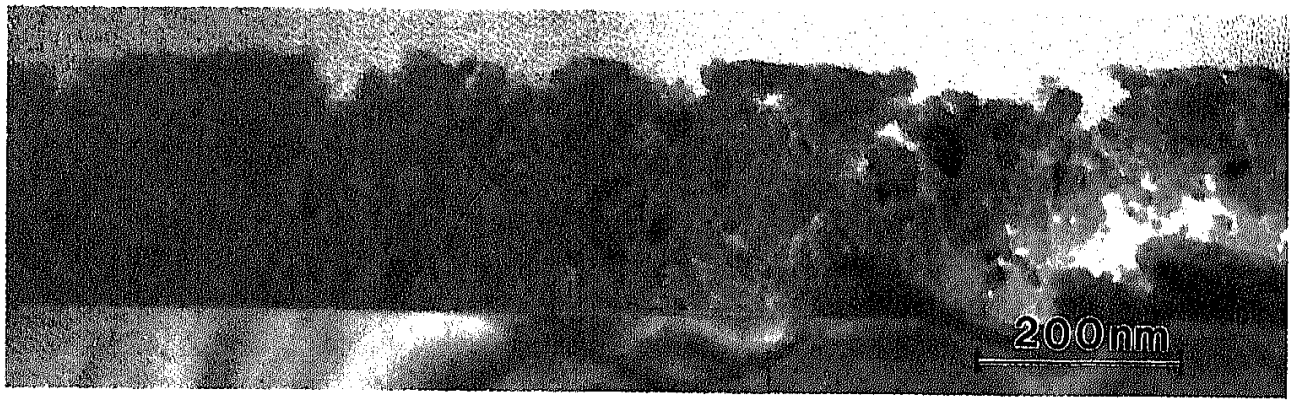

Fig. 6. TEM cross-section of an ITO film sputtered at $p[O_2] = 0.1 \times 10^{-1}$ Pa

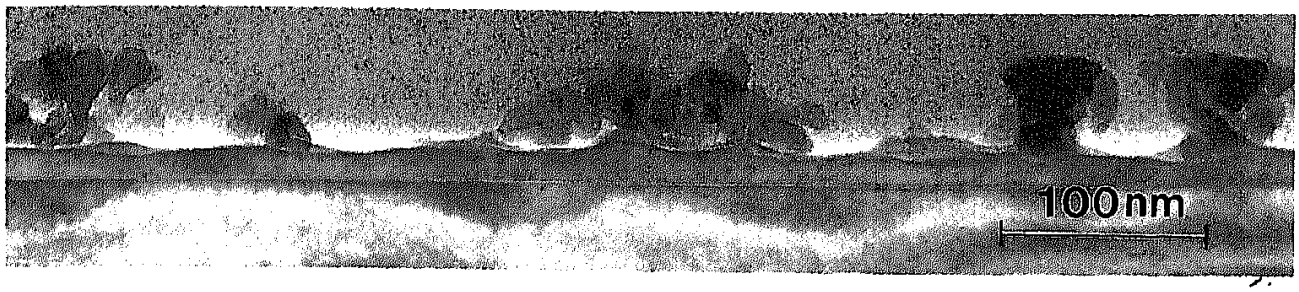

Fig. 7. Polycrystalline ITO film after prolonged exposure to etching agent

until it has reached a constant value after some 5 min. Then, during the deposition run, the voltage rises slowly. This means that the sputtering rate decreases while the film is growing. The oxygen flow is held constant during a sputter run. Hence the balance between the amount of sputtered metal and oxygen depends on the sputtering rate. The lower part of a film is deposited at a higher rate than the upper part. Therefore, as discussed in Section 3.2., the film starts growing as an oxygen-poor material with an amorphous structure. Then, if the oxygen partial pressure is held above a critical value, oxygen-rich grains emerge in its upper part.

Pre-sputtering should be performed very thoroughly, but it consumes major parts of the target material. So for reasons of economy, the pre-sputtering time cannot be extended beyond the duration of one sputtering run.

3.4 Etching properties

A specific problem arising in the use of ITO for large-area microelectronics applications is the need for structuring ITO films by photolithography. Since lift-off processes are not always desirable[2]), an ITO material must be produced that can easily be patterned by wet-chemical etching. Only those etching agents may be applied that do not attack the parts of the device that are used underneath the ITO layer. In the case of image sensors, a chromium electrode and an a-Si:H film are present. Therefore, neither nitric acid nor alkaline solutions can be used. With H_2SO_4, only low etching rates could be obtained. HCl turned out to be suitable for etching ITO, since it does not attack the chromium strip lines that are covered with a native chromium oxide layer.

The etching rate of ITO samples is rather low. Although a correlation with the deposition rate is visible (Fig. 9), the values scatter from one sample to another in an irregular manner. ITO films that are bulk crystalline cannot be etched at all, even after exposure to 10% HCl for several hours. Samples with a dense crystalline overlayer are also hardly etchable, whereas porous films or films consisting of small grains embedded in an amorphous matrix offer a good opportunity for the acid to attack the material, thus resulting in a high etching rate.

The required pattern resolution is in the order of 2 to 5 μm. Therefore, only small underetching of the resist mask is tolerable. The ITO layers described above show rather strong underetching which may exceed several μm. This makes it impossible to produce fine patterns photolithographically. An alternative deposition scheme was thus proposed [21]. During the sputtering process, the oxygen partial pressure is varied periodically. Details

---

[2]) It is difficult to perform a photolithographical lift-off process homogeneously on a large area, i.e. 25×25 cm^2.

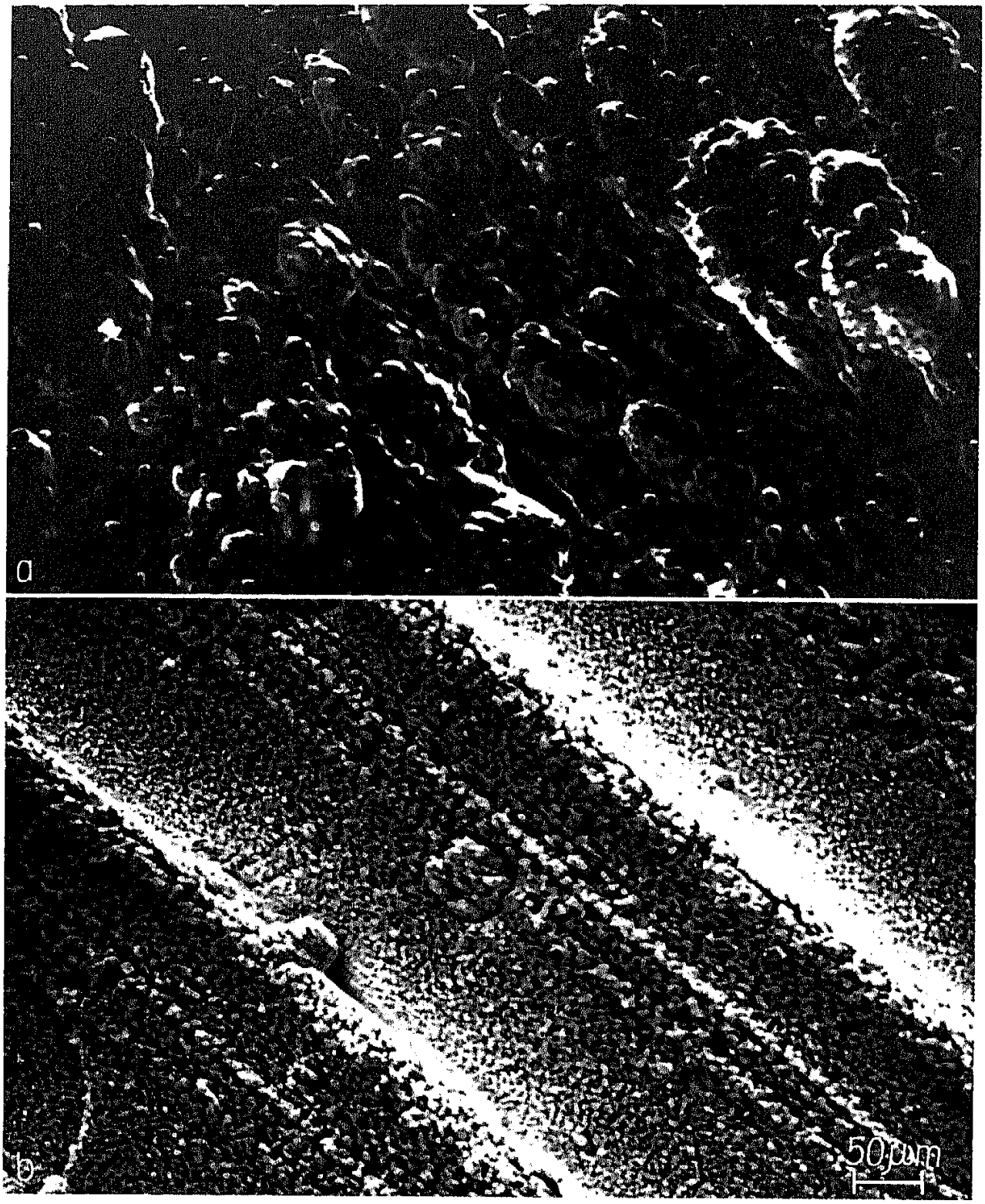

Fig. 8. SEM image of an In/Sn target (90%/10%) after 35 h sputtering: a) bottom of the sputtering crater, b) outside the sputter crater

have been published elsewhere [21]. However, ITO films produced by this method show no distinct layered structure (Fig. 10). The microstructure consists of grains with thin regions of amorphous material in-between.

Surprisingly, these "multilayer" ITO films can be deposited with much better reproducibility. The sheet resistance is 600 Ω, the optical transmission exceeds 85% and the

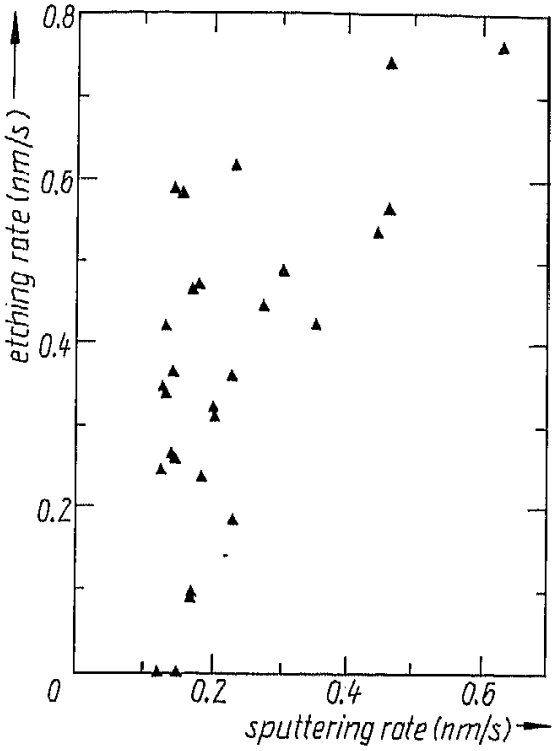

Fig. 9. Etching rate vs. sputtering rate of various ITO films

etching rate in HCl amounts to 3 nm/s. This method allows very well defined structures to be etched (Fig. 11) where lateral underetching can be kept below 200 nm.

4. Discussion

Extensive TEM investigations of differently fabricated ITO layers showed a strong correlation between the microscopic features of ITO and macroscopic properties such as etchability, optical transmission, and electrical sheet resistance. A restricted reproducibility of the ITO sputter technique can be clearly attributed to a small drift of the operating point on the characteristic resulting in large variations of the film properties. Amorphous oxygen-poor ITO layers turn out to have a high etching rate, low electrical resistance and poor optical transmission because of the intermetallic character of this material. On the other hand, compact polycrystalline films are almost unetchable and exhibit an intermediate sheet resistance combined with a high transmission due to the conducting behavior of

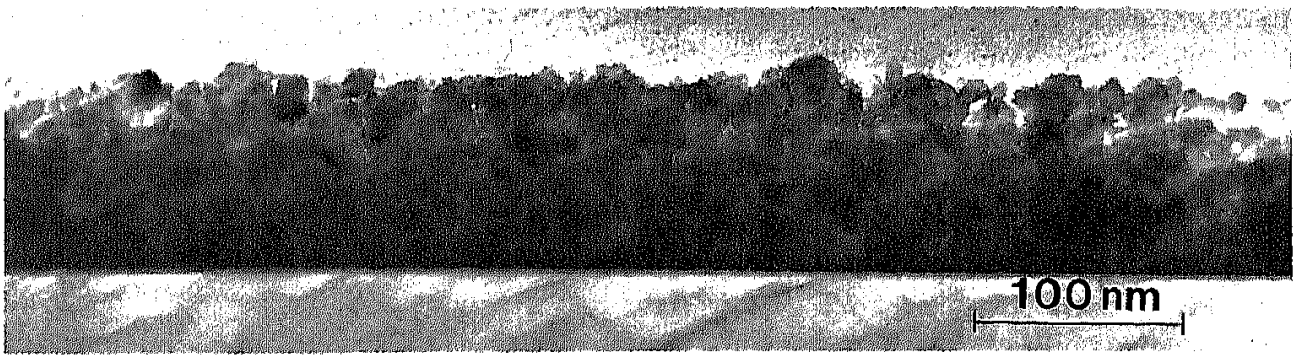

Fig. 10. TEM cross-section of an ITO film deposited with periodically varied oxygen partial pressure. The film consists of grains with small amount of amorphous material in-between. The layered deposition sequence is not visible in the microstructure

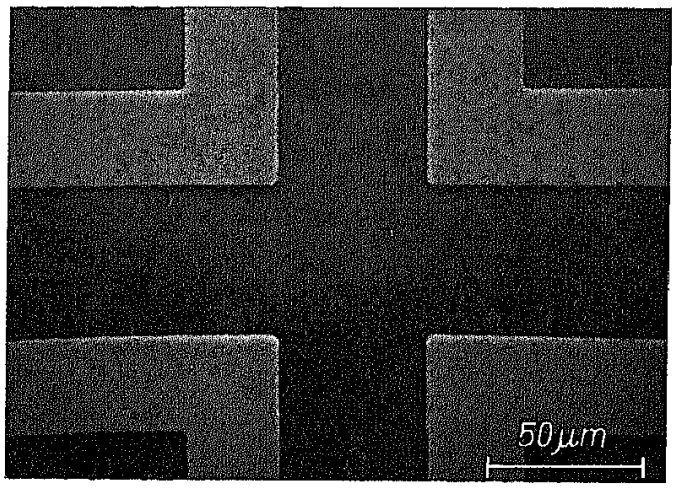

Fig. 11. SEM image of an etched structure in an ITO film

transparent In_2O_3 [5, 16]. Crystalline ITO penetrated by vertical channels shows a sufficiently high etching rate, a high electrical resistance and an intermediate optical transmission. The difference to compact crystalline films can be unterstood by the formation of the honeycomb-like vertical channel system acting as a barrier for charge carriers travelling within the film plane and leading to an increase in resistivity. The channels also cause scattering inhomogeneities for optical photons, thus resulting in reduced transparency. The higher etching rate for porous crystalline material compared with compact ITO can be explained by penetration of the etching agent into the vertical channels, accompanied by lateral etching at the mostly amorphous bottom part of the film, thus finally lifting off larger conically-shaped ITO grains whose apices are near the bottom of the film.

The oxidation of the target which normally takes place during ITO sputtering leads to a decrease of the sputtering rate and thus to an accumulation of oxygen. Therefore, the oxygen fraction relative to that of indium and tin is enhanced, yielding oxygen-rich films with a polycrystalline microstructure. Accordingly, pre-sputtering is important in order to produce a metallic target surface for a well-defined initial condition.

With knowledge of these complicated interactions between microscopic features and macroscopic data, a new "multilayer" deposition scheme was recently proposed for ITO films [21]. These films exhibit a high etching rate, since they consist of very small crystallites imbedded in an amorphous matrix. Since crystalline ITO turned out to be almost unetchable, the etching agent can dissolve the amorphous part of the film, thus lifting off the grains. To explain the formation of such finely grained material, we suggest the following model. Sputtering an oxygen-poor "layer" leads to an almost metallic amorphous phase on the substrate. As we found during other experiments, a sputtered metallic indium–tin alloy tends to coalesce to small amorphous islands. Therefore, sputtering in an oxygen-poor ambient leads to an amorphous porous phase. Oxygen-rich ITO normally forms a uniform crystalline layer. The oxygen-poor islands inhibit the growth of a continuous crystalline film. Consequently, many grains several nm in size start to grow in oxygen-rich ambient and are separated by amorphous material and numerous pores during the following oxygen-poor growth.

Since the metal-rich islands form only a small fraction of the film, they influence its transparency only slightly. On the other hand, these islands are etched very fast, as described above. The resistivity is sufficiently low because of the intermediate conductivity of ITO grains and the low resistivity of the amorphous phase as discussed above.

5. Conclusions

ITO films prepared by reactive dc magnetron sputtering can be produced with properties that make this material useful for application in opto-electronic devices. Nevertheless, certain restrictions arise from the material itself and from the sputtering process. ITO films that exhibit the desired values of conductivity and transparency require an oxygen partial pressure in the sputtering ambient that must be kept within very narrow limits. Good process control and reproducible starting conditions for every sputtering run are required to obtain films of constant quality.

The sheet resistance can be kept below 1 kΩ, which is low enough for image sensor applications, as signal currents are of the order of 10 $\mu A/cm^2$ or less. Solar cells call for transparent electrodes with much higher conductivities since the output current is many orders of magnitude higher ($>10\ mA/cm^2$). Producing ITO with lower resistivity would require a higher annealing temperature for the ITO films that cannot be applied to devices with ITO as a top electrode. ITO as a bottom electrode for devices based on a-Si:H may lead to indium diffusion into the semiconductor, especially at higher deposition temperatures of the a-Si:H [23]. This deteriorates the quality of the a-Si:H markedly. Hence the application of our ITO films for solar cells, if desired, would need further development.

The transparency of the ITO films is excellent, with values of up to 90%, keeping in mind that the samples were not annealed in excess of 200 °C. The reflectivity losses can be reduced considerably when the layer thickness is adjusted to the wavelength of the light used in a specific application, i.e. the ITO serves as an antireflective layer.

The etching properties, i.e. etching rate, underetching, and reproducibility, can be enhanced by simply modulating the oxygen partial pressure during sputtering. This leads to a porous, partial amorphous microstructure of the ITO films without affecting the optical or electrical properties.

To produce ITO films with specified properties, it is important to control the microstructure of the growing film. A favorable microstructure should consist of grains imbedded in an amorphous matrix.

Acknowledgements

We would like to thank W. Müller for running the sputtering machine, and S. Heller for taking the SEM images during the work for her Diplom Thesis.

References

[1] D. E. Carlson, in: Semiconductors and Semimetals, Vol. 21, Part D, Ed. J. I. Pankove, Academic Press, 1984 (p. 7).
[2] K. Kempter, Proc. SPIE **617**, 120 (1986).
[3] M. Hoheisel, G. Brunst, and H. Wieczorek, J. non-crystall. Solids **90**, 243 (1987).
[4] D. G. Ast, see [1] (p. 115).
[5] K. L. Chopra, S. Major, and D. K. Pandya, Thin Solid Films **102**, 1 (1983).
[6] M. Hoheisel, N. Brutscher, and H. Wieczorek, J. appl. Phys. **66**, 4466 (1989).
[7] M. Hoheisel, N. Brutscher, and H. Wieczorek, J. non-crystall. Solids **115**, 114 (1989).
[8] M. Hoheisel, N. Brutscher, H. Oppolzer, and S. Schild, J. non-crystall. Solids **97/98**, 959 (1987).
[9] I. Hamberg and C. G. Granqvist, J. appl. Phys. **60**, R123 (1986).
[10] M. Buchanan, J. B. Webb, and D. F. Williams, Thin Solid Films **80**, 373 (1981).

[11] A. G. SPENCER, R. P. HOWSON, and R. W. LEWIS, Thin Solid Films **158**, 141 (1988).
[12] G. BRADSHAW and A. J. HUGHES, Thin Solid Films **33**, L5 (1976).
[13] T. RATCHEVA and M. NANOVA, Thin Solid Films **141**, L87 (1986).
[14] S. HELLER, Diploma Work, Technische Universität München, 1990.
[15] S. YAMAMOTO, T. YAMANAKA, and Z. UEDA, J. Vacuum Sci. Technol. A **5**, 1952 (1987).
[16] A. DIETRICH, Thesis, Universität Regensburg, 1980.
[17] S. BERG, H.-O. BLOM, T. LARSSON, and C. NENDER, J. Vacuum Sci. Technol. A**5**, 202 (1987).
[18] T. LARSSON, H.-O. BLOM, C. NENDER, and S. BERG, J. Vacuum Sci. Technol. A**6**, 1832 (1988).
[19] A. MITWALSKY, M. HOHEISEL, W. MÜLLER, and C. MROTZEK, Inst. Phys. Conf. Ser. No. 93, Vol. 2, Chap. 3, 1988 (p. 107).
[20] L. GUPTA, A. MANSINGH, and P. K. SRIVASTAVA, Thin Solid Films **176**, 33 (1989).
[21] M. HOHEISEL, S. HELLER, C. MROTZEK, and A. MITWALSKY, Solid State Commun. **76**, 1 (1990).
[22] T. HILLMER, internal report.
[23] P. PRAVA, M. A. PERINO, C. F. PIRRI, R. GALLONI, and A. CARNERA, J. Vacuum Sci. Technol. A 7, 1318 (1989).

(Received November 27, 1990)